Rubidium isotopic composition of the Earth, meteorites, and the Moon: Evidence for the origin of volatile loss during planetary accretion

Emily Pringle, Frédéric Moynier

CrossMark

Rubidium isotopic composition of the Earth, meteorites, and the Moon: Evidence for the origin of volatile loss during planetary accretion

Emily A. Pringle [a], Frédéric Moynier [a,b,*]

[a] *Institut de Physique du Globe de Paris, Sorbonne Paris Cité, Université Paris Diderot, CNRS, 75005 Paris, France*
[b] *Institut Universitaire de France, Paris, France*

ABSTRACT

Understanding the origin of volatile element variations in the inner Solar System has long been a goal of cosmochemistry, but many early studies searching for the fingerprint of volatile loss using stable isotope systems failed to find any resolvable variations.

An improved method for the chemical purification of Rb for high-precision isotope ratio measurements by multi-collector inductively-coupled-plasma mass-spectrometry. This method has been used to measure the Rb isotopic composition for a suite of planetary materials, including carbonaceous, ordinary, and enstatite chondrites, as well as achondrites (eucrite, angrite), terrestrial igneous rocks (basalt, andesite, granite), and Apollo lunar samples (mare basalts, alkali suite). Volatile depleted bodies (e.g. HED parent body, thermally metamorphosed meteorites) are enriched in the heavy isotope of Rb by up to several per mil compared to chondrites, suggesting volatile loss by evaporation at the surface of planetesimals. In addition, the Moon is isotopically distinct from the Moon in Rb. The variations in Rb isotope compositions in the volatile-poor samples are attributed to volatile loss from planetesimals during accretion. This suggests that either the Rb (and other volatile elements) were lost during or following the giant impact or by evaporation earlier during the accretion history of Theia.

1. Introduction

Although the abundance of volatile elements in the inner Solar System has important implications for the accretion and evolution of the terrestrial planets, the origin of volatile element variations in inner Solar System bodies is debated. For example, although carbonaceous chondrites (CC) constitute the most chemically primitive meteorite group, they display differing degrees of volatile element depletions (i.e. depletions in elements with a 50% condensation temperature, T_c, between 250 K and 1250 K). The CI-type CC have elemental abundances that closely match the composition of the solar photosphere (excluding Li, H, C, N, O, and the noble gases; Palme et al., 2014). The other CC classes show increasing depletions in volatile elements corresponding to increasing elemental volatility in the order CI–CM–(CO, CV)–CK (Palme et al., 2014). Hypotheses to account for these volatile element abundance variations in bulk chondrites are varied and include nebular effects (e.g. condensation or evaporation; Wasson and Chou, 1974;

Ringwood, 1966), or mixing of distinct chemical and isotopic reservoirs (Larimer and Anders, 1967).

Similarly, volatile element depletions in achondrites and in the terrestrial planets relative to CI are variable, and the origins of these variations are debated. Like undifferentiated meteorites, differentiated bodies may inherit their volatile element abundances from the processes of condensation and/or the early stages of accretion. However, differentiated bodies may also experience volatile loss through high-energy processes during the later stages of accretion and subsequent planetary evolution (e.g. evaporative loss during impacts, magma ocean degassing). The signature of these and other geochemical processes may be recorded in the isotopic compositions of planetary materials, making isotopes a key tracer of processes in the early solar system.

Rubidium is one element that is particularly well-suited to study the questions outline above. Rubidium is a moderately volatile lithophile element with a T_c of 800 K (Lodders, 2003). Due to the similar incompatibility of Rb and Sr, the Rb/Sr ratio is generally constant in planetary materials and is a useful indicator of volatile depletion since Sr ($T_c = 1455$ K) is much more refractory than Rb. The Rb/Sr variations in bodies from the inner solar system span a range of nearly four orders of magnitude (Halliday and Porcelli, 2001). Rubidium is present at a level of 1–2 ppm

in bulk chondrites (e.g. Lodders and Fegley, 1998). During partial melting, Rb is relatively enriched in crustal materials, such as terrestrial granites (∼200 ppm Rb), compared to the mantle (cf. <0.2 ppm Rb in terrestrial peridotite) (e.g. Lodders and Fegley, 1998). Multiple bodies in the inner Solar System exhibit significant depletions in Rb compared to chondrites, including the Earth, the Moon, and achondrites from the Howardite–Eucrite–Diogenite (HED) and angrite groups. The large variations in Rb/Sr ratio and Rb concentration (denoted [Rb]) in these planetary materials may hold important clues to the mechanism of volatile element depletion in the inner Solar System.

Rubidium is comprised of two isotopes: the stable isotope ^{85}Rb (72.165%) and the long-lived radioactive isotope ^{87}Rb (27.835%), which decays to ^{87}Sr with a half-life of 49.76×10^9 y (Nebel et al., 2011b). Mass-dependent Rb isotope variations in planetary materials are likely limited in most cases for several reasons. First, Rb is heavy compared to traditional stable isotope systems (e.g. C, N, O, S) so the relative mass difference between the two Rb isotopes is small. Second, Rb exists only as Rb$^+$ and therefore no isotopic fractionation occurs during partitioning between phases with differing valence states (e.g. as for Fe between Fe(II) and Fe(III)). Third, equilibrium isotope fractionation due to partitioning between phases is generally larger for species among covalent bonds, but Rb has an ionic bonding character. Despite these reasons, large mass-dependent variations may occur during evaporation due to the volatile nature of Rb. The pioneer study on Rb isotopes in chondrites (Nebel et al., 2011a) found generally similar Rb isotope compositions between the Earth and chondrites, but with a relatively large analytical uncertainty of 0.2‰. It is possible that improvements in precision may allow the identification of small variations in Rb isotope compositions. Finally, the geochemical relationship between Rb and K makes the further study of Rb timely: although early studies on K isotope cosmochemistry did not find resolvable K isotope variations (Humayun and Clayton, 1995), recent work has uncovered a small difference between the K isotope composition of the Earth and the Moon (Wang and Jacobsen, 2016a, 2016b).

Here we present a new method for the chemical separation of Rb for high-precision isotope ratio measurements by multi-collector inductively-coupled-plasma mass-spectrometer (MC-ICP-MS). This method is used to report new Rb isotope data for a broad suite of planetary materials, including chondrites from the Carbonaceous (CC), Ordinary (OC), and Enstatite (EC) groups, achondrites (eucrite, angrite), terrestrial igneous rocks (basalt, andesite, granite), and Apollo lunar samples (basalt, alkali suite). The goal of this work is to present an updated overview of Rb isotope variations in the inner Solar System and to provide an initial assessment of the possible causes of any variations.

2. Samples and methods

2.1. Samples

A variety of terrestrial samples were selected in order to gain insight into the behavior of Rb during igneous differentiation. The terrestrial rocks used in this study include one granite (GS-N), one andesite (AGV-2), and four basalts. The basalts include samples from a variety of settings: one Columbia River continental flood basalt (BCR-2), one Mid-Ocean Ridge Basalt (MORB) from the mid-Atlantic ridge (EW9309 10D), and Ocean Island Basalts (OIB) from Hawaii (BHVO-2) and Galapagos (AHANEMO2 D20B).

Meteorite samples were selected from a variety of groups to achieve an overview of Rb isotope variations in the inner Solar System. This study focuses on observed meteorite falls when possible in order to avoid the effects of terrestrial weathering on Rb isotope compositions. The chondrites used in this study include

the CC Orgueil (CI1), Murchison (CM2), Cold Bokkeveld (CM2), Felix (CO3.3), Lancé (CO3.3), Allende (CV3, oxidized type), Vigarano (CV3, reduced type), and Karoonda (CK4). Other chondrites analyzed include the unequilibrated OC Krymka (LL3.2) and the EC Abee (EH4), Indarch (EH4), and Khaipur (EL6). In addition, two thermally metamorphosed CM2 were selected (PCA 02012 and PCA 02010). These samples display indicators of significant volatile loss suggesting that they have been heated to temperature of ∼900 °C (Nakato et al., 2013; Beck et al., 2014).

A primary goal of this work was to investigate the Rb isotope composition of volatile-depleted bodies, including HED meteorites, angrites, and lunar basalts. The achondrites analyzed include two HED meteorite falls: the monomict eucrites Juvinas and Stannern. One angrite, SAH99555, was also measured for Rb isotope composition.

The comprehensive suite of Apollo mission lunar basalts includes two low-Ti olivine basalts (12012, 15555), one low-Ti ilmenite basalt (12016), one low-Ti low-K ilmenite basalt (10003), two low-Ti high-K ilmenite basalts (10017, 10057). One Alkali suite cataclastic norite (77215) from Apollo 17 was also selected for Rb isotope analysis.

2.2. Chemical purification of Rb

Whole rock samples were crushed by hand using an agate mortar until a fine powder was obtained. A minimum of 0.5 g of terrestrial rock or meteorite and 100 mg of lunar samples was crushed in order to avoid non-representational sample analysis. An aliquot of ≤125 mg of powdered sample was weighed depending on the Rb concentration of the sample; masses were calculated to yield >20 ng Rb for isotope ratio measurements. Sample powders were digested using a mixture of concentrated HF/HNO$_3$ and heated at 130 °C in closed Teflon bombs for >48 h. After evaporation of the HF/HNO$_3$, 6N HCl was added and the samples were again heated at 130 °C to achieve dissolution of fluoride complexes. Samples were then evaporated to complete dryness and were ready for chemical purification.

Previous work on Rb isotopes utilized Zr doping for correction of mass bias on Rb (Nebel et al., 2005, 2011a). The goal of this study was to develop an improved chemical purification procedure to avoid the necessity of doping and improve analytical precision. To that end, a multi-step column chemistry procedure was developed in order to ensure complete separation of Rb from matrix elements and quantitative recovery of Rb (see Supplementary materials for additional discussion of the methods developed by this work). This chemistry achieves efficient separation of Rb from elements with isobaric and molecular interferences (in particular ^{87}Sr from ^{87}Rb, but also double-charged Er or Yb isotopes), on mass/charge of interest (84, 85, 86, 87, 88; Sr isotopes are monitored for the correction of ^{87}Sr on ^{87}Rb). A major focus was sufficient removal K to avoid any potential matrix effects on the measured Rb isotope compositions (see supplementary materials).

Samples were first subjected to a Ca removal step using Eichrom normal DGA resin (50–100 μm). Following digestion, samples were dissolved in 1N HNO$_3$ and loaded on BioRad Poly-Prep chromatography columns containing 1.8 mL conditioned DGA resin; Rb was collected by washing with 1N HNO$_3$ while >90% Ca was effectively retained by the resin. Our tests have shown that this is an important step to avoid two adverse effects caused by Ca: first, Ca may change the shape and placement of the Rb peak on cation exchange resin; this can lead to either loss of Rb (i.e. not collecting full Rb cut) or the presence of Ca in Rb cut (see supplementary materials).

After the Ca removal step, the collected sample was evaporated to dryness and the residue was dissolved in 3N HCl. The Rb was separated from matrix elements using cationic resin in three suc-

Table 1
Typical running conditions for the Neptune Plus MC-ICP-MS.

Parameter	Setting
RF power	1200 W
Cool gas	16 L/min
Aux gas	1.01 L/min
Sample gas	1.03 L/min
Peristatic pump	5 rpm
Sample cone	Jet
Skimmer cone	H
Extraction voltage	−2000 V

Table 2
Cup configuration for the Neptune Plus MC-ICP-MS.

Cup	L2	L1	C	H1	H2
Mass	84	85	86	87	88
Isotope(s)	^{84}Sr	^{85}Rb	^{86}Sr	^{87}Rb, ^{87}Sr	^{88}Sr

cessive steps to achieve an increasingly finer separation of Rb from other elements. The first and second steps utilized 3N HCl and BioRad AG50 X12 200–400 with 20 mL of resin (BioRad Econo-Pac columns) and 10 mL of resin (PP chromatography column with 0.8 cm inner diameter, 10 cm length), respectively. The collected Rb fractions were evaporated between each column pass. The final column step used 0.5N HCl and 1 mL of BioRad AG50 X8 200–400 resin (homemade PTFE column with 0.6 cm inner diameter, 3.5 cm length). The final Rb cut was evaporated and then dissolved in 0.1N HNO$_3$ for MC-ICP-MS analysis. This chemical purification procedure reduces K/Rb by a factor of 200 (to yield final K/Rb < 2) and results in final ^{88}Sr/^{85}Rb < 0.005; neither K nor Sr has any resolvable effect on measured Rb isotope compositions under these conditions (see supplementary materials for further discussion). Although the full column procedure developed by this work is long and requires large volumes of acid, the benefit is a >5× improvement in analytical precision compared to previous work (Nebel et al., 2011a).

2.3. Mass spectrometry

Rubidium isotope ratio measurements were made on the Thermo Scientific Neptune Plus MC-ICP-MS at the Institut de Physique du Globe in Paris. Samples were introduced using an ESI PFA MicroFlow nebulizer (flow rate: 100 μL/min) into either a quartz cyclonic spray chamber or an APEX desolvating sample introduction system to increase measurement sensitivity. Sample solutions were prepared to yield Rb concentrations of 10 ppb when using the spray chamber and 4 ppb when using the APEX. At these concentrations, a beam intensity of ∼1.0 V was measured on ^{85}Rb using 10^{-11} Ω resistors and under typical MC-ICP-MS running conditions (Table 1). High Rb beam intensities were found to lead to memory effects and were therefore avoided. Measurements were made in static mode using the cup configuration shown in Table 2 with the instrument operating in low-resolution. A typical mass scan of the Rb peak is shown in the supplementary materials (Fig. S1). Strontium was monitored using the ^{88}Sr ion beams. Instrumental background was measured at the beginning and throughout each analytical session (typically <1 mV on ^{85}Rb); sample measurements were subjected to a blank correction using these background measurements. The low Rb beam intensity (≤1 V) coupled with a 3 min wash times between samples were sufficient to prevent memory effects over the duration of an analytical session (typically 12–24 h). Total procedural blank for the sample preparation and chemical purification was <0.04 ng Rb, an amount corresponding to less than 0.05% of the Rb contained in a sample aliquot.

Isotope ratios were measured using blocks of 20 cycles with 8.389 s integration times; any ratio outside 2σ was discarded. Measurements were made using standard-sample bracketing to correct for instrumental mass bias. The NIST SRM984 RbCl standard was used as the bracketing standard for most sample measurements. The terrestrial basalt geostandard BCR-2 was used as alternative bracketing standard in some analytical sessions. Rubidium isotope compositions are expressed relative to the bracketing standard (either SRM984 or BCR-2) using the following delta notation:

$$\delta^{87}\text{Rb} = \left[\left(^{87}\text{Rb}/^{85}\text{Rb} \right)_{\text{sample}} / \left(^{87}\text{Rb}/^{85}\text{Rb} \right)_{\text{standard}} - 1 \right] \times 1000.$$

(1)

Reported isotope ratios are averages of repeated measurements of each sample when multiple analyses were possible. Errors are determined from repeated measurements; the 2 standard error (2 se) is reported unless stated otherwise. For the samples that have been analyzed less than 3 times, the largest 2 se reported for a sample analyzed multiple times has been used.

A variety of steps were taken to ensure robust Rb isotope measurements were obtained. First, an aliquot of the bracketing standard (SRM984) was passed through the complete chemical procedure to test if the column chemistry induced any Rb isotope fractionation. The results of this test are shown in Table 3. The standard passed through the chemistry is identical within error to the standard before chemistry (δ^{87}Rb = 0.00 ± 0.03‰), confirming that no isotope fractionation is caused by the Rb purification procedure. One sample (Allende) was analyzed in duplicate splits from the same powder aliquot, including the full dissolution and chemical purification procedure; the Allende replicates are identical within error (δ^{87}Rb = 0.12 ± 0.02‰ and δ^{87}Rb = 0.14 ± 0.04‰). In addition, a pure Rb ICP-MS solution was analyzed as an external standard during each analytical session to monitor the reproducibility of Rb isotope measurements; the long-term reproducibility was ±0.01‰ ($n = 40$). Finally, in almost all cases, sample solutions were analyzed over multiple analytical sessions and were measured using both the spray chamber and the APEX sample introduction systems as an added confirmation of the results. No difference in δ^{87}Rb was observed between the two sample introduction systems, with the exception that the APEX routinely yielded lower precisions (by ∼0.03‰).

3. Results

The Rb isotope data obtained for terrestrial samples relative to SRM984 are presented in Table 3 and Fig. 1. The terrestrial rocks measured in this study define a narrow range of δ^{87}Rb, from −0.09‰ to −0.16‰. The terrestrial basalts span nearly the entire range defined by all terrestrial samples (δ^{87}Rb range from −0.09‰ to −0.14‰). The Galapagos OIB and the MORB have identical δ^{87}Rb values within error despite the difference in degree of partial melting (degrees of ∼10–15% for MORB but lower degrees for OIB; Hofmann, 2003). The MORB (EW9309, δ^{87}Rb = −0.10 ± 0.06) and the granite (GS-N; δ^{87}Rb = −0.14 ± 0.01) represent a range in Rb concentration (denoted [Rb]) of more than two orders of magnitude, but there is no resolvable difference in their Rb isotope composition. The average obtained by analysis of all terrestrial rocks in this study is δ^{87}Rb = −0.12 ± 0.06 (2 sd).

The δ^{87}Rb values for chondritic meteorites (see Table 3 and Fig. 1) span a wider range than that measured for terrestrial rocks. The group averages for CC (δ^{87}Rb = 0.02 ± 0.25‰, 2 sd) and EC (δ^{87}Rb = −0.03 ± 0.21‰, 2 sd) are similar, while the single OC measured in this study is significantly offset from these averages (δ^{87}Rb = −0.37 ± 0.01‰). In detail, the CC have progressively lower δ^{87}Rb values in the order CI (Orgueil, δ^{87}Rb =

Table 3
Rb isotope compositions of terrestrial, lunar, and meteoritic material relative to SRM984.

Sample	Type	Find/fall	δ^{87}Rb	2 sd[a]	2 se[b]	n[c]	[Rb] (ppm)
SRM984[d]			0.00	0.07	0.03	4	
ICP			−0.12	0.08	0.01	40	
Terrestrial							
BHVO2	Basalt		−0.09	0.05	0.02	10	9.8
BCR-2	Basalt		−0.14	0.12	0.04	9	48
AHANEMO2 D20B	OIB (Galapagos)		−0.10	0.07	0.02	9	5.5
EW9309 10D	MORB (MAR)		−0.10	0.06		2	1.0
AGV-2	Andesite		−0.16	0.12	0.04	8	68.6
GS-N	Granite		−0.14	0.02	0.01	3	183
Average-terrestrial			**−0.12**	**0.06**		**6**	
Lunar							
12012	Low Ti ol. basalt		0.08	0.01		2	0.64
15555	Low Ti ol. basalt		0.07	0.07	0.03	5	0.7
12016	Low Ti il. basalt		0.02	0.08	0.04	3	0.6
average Low Ti			0.06	0.07		3	
10003	High Ti il. basalt (low K)		0.14	0.08	0.05	3	0.64
10017	High Ti il. basalt (high K)		−0.05	0.08	0.04	5	5.6
10057	High Ti il. basalt (high K)		0.06	0.13	0.06	5	5.0
average High Ti			0.05	0.19		3	
77215	Alkali suite cataclastic norite		0.02	0.08	0.04	5	3.5
Average-lunar			**0.05**	**0.12**		**7**	
Carbonaceous chondrites							
Orgueil	CI1	fall	0.19	0.13	0.06	5	2.0
Murchison	CM2	fall	0.02	0.03	0.02	5	1.6
Cold Bokkeveld	CM2	fall	−0.02	0.10	0.05	5	1.6
PCA 02012	CM2	find	2.12	0.19	0.07	7	0.9
PCA 02010	CM2	find	8.59			1	0.2
Felix	CO3.3	fall	−0.06	0.02		2	1.23
Lancé	CO3.5	fall	−0.03	0.08	0.03	7	1.4
Allende I	CV3	fall	0.12	0.04	0.02	3	1.2
Allende II	CV3	fall	0.14	0.09	0.04	5	1.2
average Allende			0.13	0.03		2	1.2
Vigarano	CV3	fall	−0.10	0.07	0.03	6	1.04
Karoonda	CK4	fall	−0.22	0.05	0.03	3	0.64
Average-carbonaceous chondrites[e]			**0.02**	**0.25**		**10**	
Ordinary chondrites							
Krymka	LL3.2	fall	−0.37	0.02	0.01	3	2.2
Enstatite chondrites							
Abee	EH4	fall	−0.01	0.08	0.03	5	3.4
Indarch	EH4	fall	−0.14	0.09	0.03	7	3.1
Khaipur	EL6	fall	0.07	0.11	0.05	5	0.77
Average-enstatite chondrites			**−0.03**	**0.21**		**3**	
Achondrites							
Juvinas	Eucrite (mm)	fall	1.51			1	0.2
Stannern	Eucrite (ST, mm)[f]	fall	0.55	0.12	0.05	5	0.56
SAH 99555	Angrite	find	0.12	0.03	0.02	3	0.4

[a] 2 sd = 2 × standard deviation.
[b] 2 se = 2 × standard deviation/$\sqrt{n}$.
[c] n = number of measurements.
[d] Rb standard passed through column chemistry.
[e] Excluding PCA02012 and PCA02010.
[f] ST = Stannern trend eucrite and mm = monomict breccias.

0.19 ± 0.06‰), CM (on average, δ^{87}Rb = 0.00 ± 0.05, 2 sd), CO (on average, δ^{87}Rb = −0.05 ± 0.04‰), CV (Vigarano, δ^{87}Rb = −0.10 ± 0.03‰), and CK (Karoonda, δ^{87}Rb = −0.22 ± 0.03‰). The oxidized-type CV3 Allende is a notable exception, with a replicate average value of δ^{87}Rb = 0.13 ± 0.02. This may be due to inherent sample heterogeneity in Rb isotope composition, as observed by Nebel et al. (2011a). The values for EH are similar on average (δ^{87}Rb = −0.08 ± 0.19‰, 2 sd) to those of terrestrial rocks within error, although the EL6 Khaipur (δ^{87}Rb = 0.07 ± 0.05‰) is shifted toward a heavier Rb isotope composition compared to the BSE.

The heated CM chondrites and the achondrites display significant δ^{87}Rb variations, with ^{87}Rb enrichments of up to nearly 10 per mil compared to other chondritic meteorites (see Table 3 and

Fig. 2). The largest Rb isotope variations measured in this study are observed in the heated CM, PCA 02010 (δ^{87}Rb = 8.59‰) and PCA 02012 (δ^{87}Rb = 2.12 ± 0.07‰). The eucrites Juvinas (δ^{87}Rb = 1.51‰) and Stannern (δ^{87}Rb = 0.55 ± 0.05‰) also display significant enrichments in ^{87}Rb compared to primitive (i.e. non-heated) chondrites. The heated CM PCA02010 and Juvinas represent the samples with the lowest [Rb] measured in this study, at 0.2 ppm for both samples. Due to the limited amount of Rb, only one analysis was possible for each of these samples. However, the heated CM PCA02012 contained sufficient Rb for multiple measurements (notably over multiple analytical sessions); the positive δ^{87}Rb values for this sample were well reproduced by all measurements. Therefore, a precision of ±0.07‰ of this sample is considered to
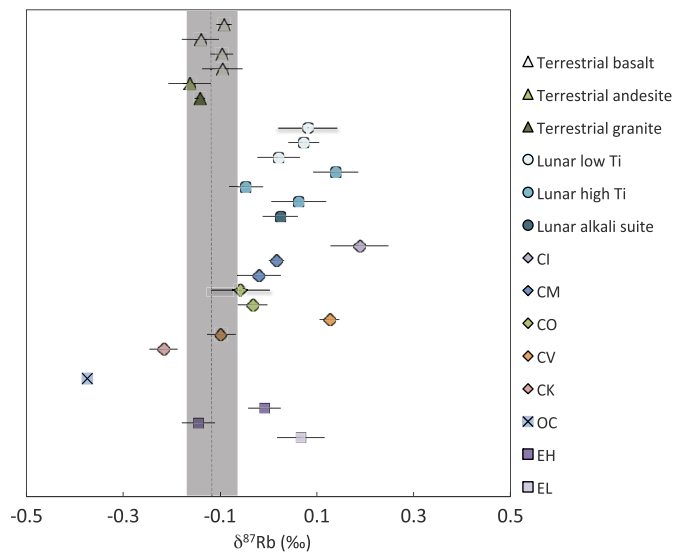
Fig. 1. Plot of δ^{87}Rb values for terrestrial and lunar rocks and carbonaceous, ordinary, and enstatite chondrites (error bars are 2 se). Terrestrial samples span a narrow range in δ^{87}Rb; the average of the terrestrial samples (± 2 sd) is indicated by dotted line and the shaded grey bar. Lunar samples are offset towards positive δ^{87}Rb values compared to terrestrial rocks. The chondrites exhibit a wider range in Rb isotope variations, with both positive and negative δ^{87}Rb values compared to terrestrial rocks. (For interpretation of the colors in this figure, the reader is referred to the web version of this article.)
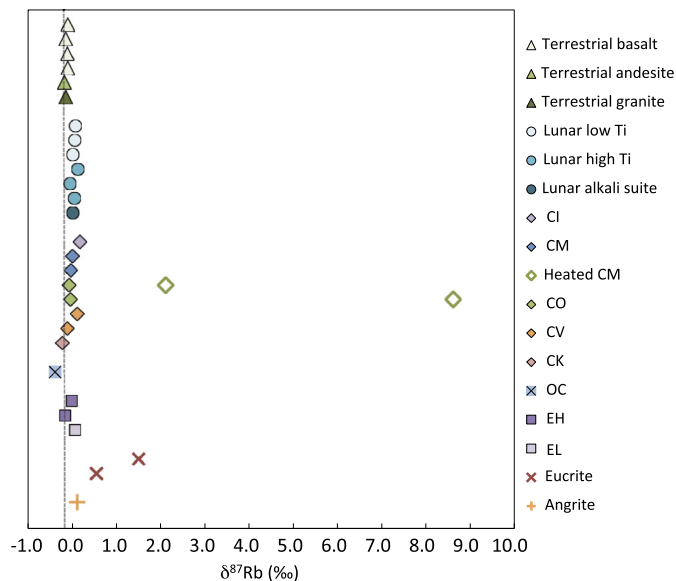

Fig. 2. Plot of δ^{87}Rb values for terrestrial rocks, lunar samples, chondrites, and achondrites (error bars are 2 se). The axis has been expanded compared to Fig. 1 in order to show the extreme positive δ^{87}Rb values measured for the heated CM chondrites, the eucrites and the angrite. Heavy Rb isotope enrichments of several per mil compared to terrestrial rocks are observed in these volatile depleted materials. (For interpretation of the colors in this figure, the reader is referred to the web version of this article.)

be representative of the precision for the Rb isotope ratio measurements of PCA 02010 and Juvinas. The single angrite measured by this study has a δ^{87}Rb value (δ^{87}Rb $= 0.12 \pm 0.02$‰) that is resolvable from terrestrial but shifted towards heavy Rb isotope compositions to only a small degree.

The Rb isotope data for lunar rocks are presented in Table 4 and Figs. 1 and 3a. Lunar samples are consistently offset towards heavier Rb isotope compositions (on average, δ^{87}Rb $= 0.05 \pm 0.12$‰, 2 sd) compared to terrestrial rocks. The averages for low-Ti lu-
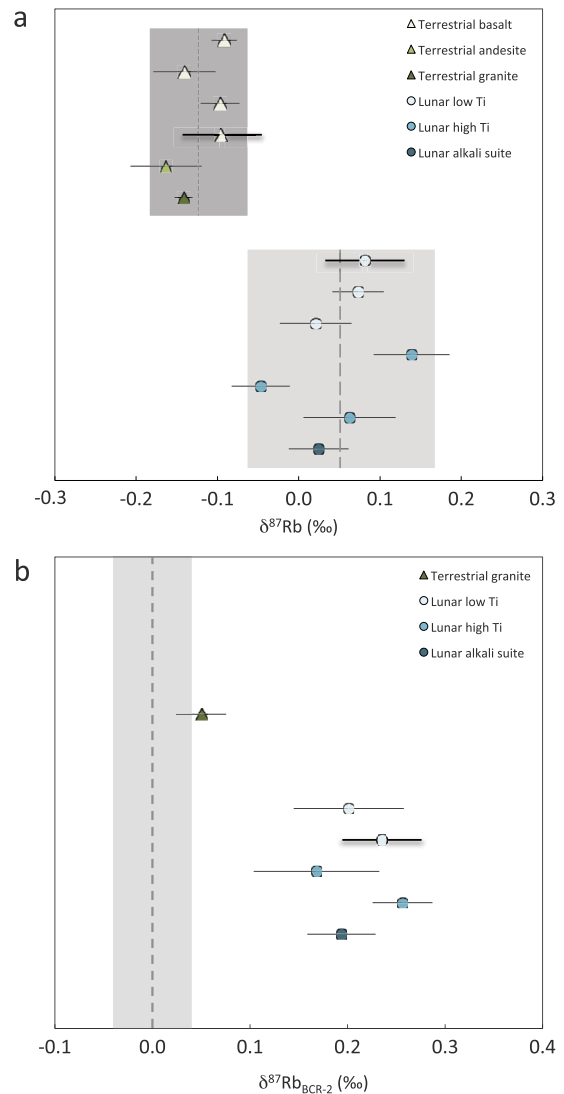

Fig. 3. (a) Detail plot of δ^{87}Rb for terrestrial and lunar rocks (error bars are 2 se). The average of the terrestrial samples (± 2 sd) is indicated by dotted line and the dark grey bar. The average of the lunar samples (± 2 sd) is shown by the dashed line and the light grey bar. There is a clear difference in δ^{87}Rb between terrestrial and lunar samples, with rocks from the Moon showing heavy Rb isotope enrichments compared to rocks from the Earth. (b) Plot of δ^{87}Rb$_{BCR-2}$ for terrestrial and lunar rocks, showing Rb isotope measurements using the terrestrial basalt BCR-2 as the bracketing standard. The δ^{87}Rb value of BCR-2 (± 2 se) is indicated by the dashed line and shaded grey box. Lunar samples are again enriched in ^{87}Rb compared to the terrestrial basalt by ~0.2‰. (For interpretation of the colors in this figure, the reader is referred to the web version of this article.)

nar basalts (δ^{87}Rb $= 0.06 \pm 0.07$‰, 2 sd) and high-Ti lunar basalts (δ^{87}Rb $= 0.05 \pm 0.19$‰, 2 sd) are similar, although more variations are present in the high-Ti basalts. The alkali suite rock, 77215, has a δ^{87}Rb value of 0.02 ± 0.04‰. The difference between the Rb isotope composition of the Moon and the BSE is denoted by Δ^{87}Rb$_{Moon-BSE} = \delta^{87}$Rb (Moon average) $- \delta^{87}$Rb (BSE average); all the lunar and terrestrial rocks measured in this study yield a value of Δ^{87}Rb$_{Moon-BSE} = 0.17 \pm 0.13$‰ (2 sd).

To confirm the heavy Rb isotope enrichments observed for the lunar samples relative to terrestrial rocks, additional measurements using the terrestrial basalt BCR-2 as the bracketing standard were performed. These measurements are denoted δ^{87}Rb$_{BCR-2}$ and are presented in Table 4 and Fig. 3b. These direct comparisons against a terrestrial basalt makes small differences easier to resolve and avoids the necessity of error propagation when comparing the δ^{87}Rb values of two different samples. The relative differ-

Table 4
Rb isotope compositions of terrestrial and lunar material relative to the terrestrial basalt BCR-2.

Sample	Type	$\delta^{87}Rb_{BCR-2}$	2 sd[a]	2 se[b]	n[c]
SRM984		0.17	0.02	0.01	2
ICP		0.12	0.07	0.05	2
GS-N	Granite	0.05	0.04	0.03	3
Lunar					
15555	Low Ti ol. basalt	0.20	0.10	0.06	3
12016	Low Ti il. basalt	0.24			1
10017	High Ti il. basalt (high K)	0.17	0.11	0.06	3
10057	High Ti il. basalt (high K)	0.26	0.05	0.03	3
77215	Alkali suite cataclastic norite	0.19	0.06	0.04	3
Average-lunar		**0.21**	**0.07**		**5**

[a] 2 sd = 2 × standard deviation.
[b] 2 se = 2 × standard deviation/$\sqrt{n}$.
[c] n = number of measurements.

ences observed between lunar samples and terrestrial rocks during bracketing by the normal Rb standard SRM984 (see Table 3 and Fig. 3a) are well reproduced in the data using BCR-2 as the bracketing standard (Table 4 and Fig. 3b). In addition, the granite GS-N was measured against BCR-2 ($\delta^{87}Rb_{BCR-2} = 0.05 \pm 0.03$‰) to confirm the homogeneity in the Rb isotope composition of terrestrial rocks. In every case, lunar samples display resolvable differences from the terrestrial rocks (both BCR-2 and GS-N), with positive shifts in $\delta^{87}Rb_{BCR-2}$. On average, the lunar samples have a value of $\delta^{87}Rb_{BCR-2} = 0.21 \pm 0.07$‰, 2 sd. This confirms that lunar basalts and BSE have distinct Rb isotope compositions.

4. Discussion

4.1. An estimate of the Rb isotope composition of the Bulk Silicate Earth

The previous study of Rb isotope in terrestrial samples (Nebel et al., 2005) and found no resolvable variation in $\delta^{87}Rb$ values outside their analytical uncertainty (± 0.5‰). This study finds a similar lack of variations in terrestrial Rb isotope variations but with a 10 times improvement in precision. The terrestrial rocks analyzed in this study define a very narrow range in Rb isotope composition, with an average $\delta^{87}Rb$ of -0.12 ± 0.06 (2 sd). Although the MORB (EW9309, $\delta^{87}Rb = -0.10 \pm 0.06$‰) and the granite (GS-N; $\delta^{87}Rb = -0.14 \pm 0.01$‰) represent differences in [Rb] of more than two orders of magnitude, there is no resolvable difference in their Rb isotope composition. In addition, basalts from a variety of geological settings, including mid-ocean ridge, intraplate plume, and continental, show no resolvable differences in $\delta^{87}Rb$. Finally, no clear trend is present between $\delta^{87}Rb$ and [Rb] across the suite of terrestrial rocks analyzed in this study (see Fig. 4), suggesting that Rb isotope fractionation during igneous differentiation is limited to less than 0.05‰. This indicates that the major reservoirs of Rb on Earth (i.e. the crust and the mantle, with $\sim$55% and $\sim$45% of the BSE Rb budget, respectively) have similar Rb isotope compositions, and that crustal rocks may be used to estimate the $\delta^{87}Rb$ of their parent body. Therefore, the $\delta^{87}Rb$ value for the Bulk Silicate Earth (BSE) is well represented by the average of terrestrial rocks measured in this study, $\delta^{87}Rb = -0.12 \pm 0.06$ (2 sd).

4.2. Rubidium isotope variations in chondrites

The chondrites analyzed in this study display small but resolvable variations in $\delta^{87}Rb$. However, since Rb has only two isotopes, it is not possible to attribute the variations in $\delta^{87}Rb$ to solely mass-dependent isotope fractionation by the measurement of Rb isotope ratios alone. Mass-independent isotope variations (such as inherited nucleosynthetic differences) would also be evident as variations in $\delta^{87}Rb$ values. However, comparisons of $\delta^{87}Rb$ values with
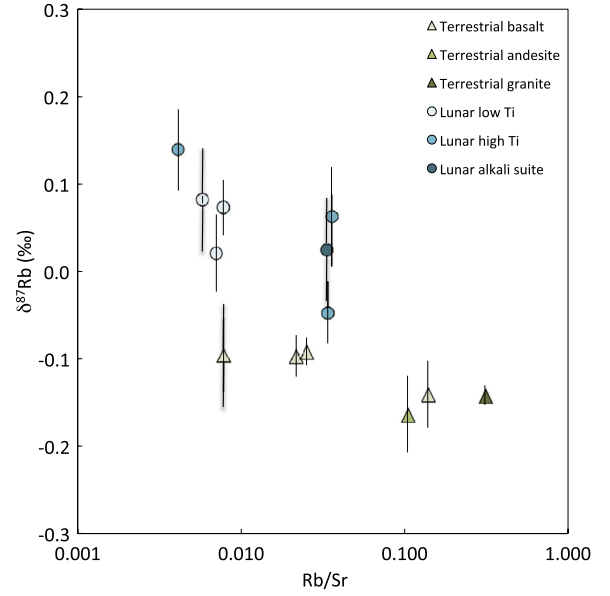
Fig. 4. Plot of $\delta^{87}Rb$ versus Rb/Sr for terrestrial and lunar samples (error bars are 2 se). Terrestrial samples do not display a clear trend between $\delta^{87}Rb$ and Rb/Sr, suggesting that Rb isotope fractionation during igneous differentiation is limited to less than 0.05‰. Lunar rocks may become slightly shifted towards positive $\delta^{87}Rb$ values with decreasing Rb/Sr ratio; however, samples with the same Rb/Sr can span a range in $\delta^{87}Rb$ of $\sim$0.1‰ so the existence of this trend is unclear. Lunar low-Ti basalts and the alkali suite sample have a narrower range in $\delta^{87}Rb$ than high-Ti basalts. (For interpretation of the colors in this figure, the reader is referred to the web version of this article.)
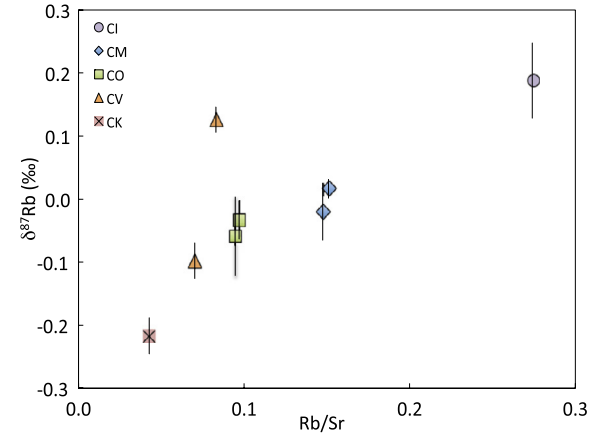
Fig. 5. Plot of $\delta^{87}Rb$ versus Rb/Sr for bulk carbonaceous chondrites, including samples from the CI, CM, CO, CV, and CK groups (error bars are 2 se). There is a trend toward light Rb isotope enrichments with decreasing Rb/Sr. This is opposite the effect expected if Rb abundance variations between CC groups was due to volatile loss of Rb. Mixing of isotopically distinct reservoirs is the most likely cause of the trend between $\delta^{87}Rb$ and Rb/Sr observed in CC.

the isotope systems of other moderately volatile elements may provide distinguishing information into the cause of the Rb isotope variations in planetary materials.

There is a relationship between $\delta^{87}Rb$ and Rb/Sr ratio between the CC measured in this study. The CC display a trend toward lighter Rb isotope composition coupled with decreasing Rb/Sr ratio (see Fig. 5). This is opposite to the effect expected if volatile element abundance variations in CC were caused by evaporation, which would produce heavy Rb isotope enrichments coupled with Rb loss if evaporation occurred under Rayleigh conditions. A similar inverse volatility trend has also been observed in bulk CC for the Zn isotope system, where mass-dependent light Zn isotope enrichments are observed with decreasing Zn (Luck et al., 2005;

Pringle et al., 2017). This relationship for Zn indicates that the volatile element abundance variations in CC are not due to evaporation or condensation, but rather are due to the mixing of chemically and isotopically distinct primordial reservoirs consisting of refractory component and a volatile-rich (CI-like) component (Luck et al., 2005; Pringle et al., 2017). The similar behavior of the two moderately volatile elements, Rb and Zn, suggests that the Rb isotope variations may also be attributed to a mixing of primordial reservoirs.

The unequilibrated OC Krymka has the lightest Rb isotope composition of all chondrites measured in this study, with δ^{87}Rb $= -0.37 \pm 0.01$. Nebel et al. (2011a) also found resolvable light isotope enrichments in OC compared to terrestrial basalts, with values ranging between 0 and $-1‰$ but no systematic variations related to type or degree of metamorphism. At this time, the δ^{87}Rb signature of OC may be attributed to either metamorphism or it may be a signature of the Rb isotope reservoir from which OC formed. The higher precision possible with our new analytical method will allow for further investigation into the nature of Rb isotope variations among OC.

The EH have a similar Rb isotope composition as the BSE, with an average of δ^{87}Rb $= -0.08 \pm 0.19‰$ (2d). The similarity in δ^{87}Rb values between EC and Earth is further confirmation that the Earth and EC were likely derived from the same isotopic reservoir (e.g. Javoy et al., 2010; Moynier and Fegley, 2015). However, the EL6 measured in this study (Khaipur, δ^{87}Rb $= 0.07 \pm 0.05‰$) is shifted toward a heavier Rb isotope composition compared to the BSE. Notably, Khaipur is depleted in Rb compared to the EH chondrites measured in this study (with [Rb] of 0.7 ppm versus 3 ppm, respectively). One EL6 analyzed by Nebel et al. (2011a) also displayed a positive δ^{87}Rb value compared to terrestrial samples. Heavy Zn isotope enrichments in EL6 have been previously attributed to thermal metamorphism on the EL6 parent body (Moynier et al., 2011); this process may be responsible for the heavy Rb isotope compositions observed in EL6 compared to other EC. These results indicate that further study into the effects of thermal metamorphism on Rb isotope compositions is warranted.

4.3. The heavy Rb isotope enrichments in achondrites and volatile loss during accretion

This is the first study to present high-precision Rb isotope data for achondrites. This work shows that there may be a strong enrichment in the heavy isotope ^{87}Rb in volatile depleted materials compared to chemically primitive meteorites. The one exception is the angrite measured in this study, SAH 99555. Although SAH 99555 has a measured δ^{87}Rb value ($0.12 \pm 0.03‰$) that is resolvable from terrestrial composition, it is within the range of chondritic compositions (although only those of the CI Orgueil and the CV Allende) despite the extreme depletions in Rb found in this sample. Unfortunately, meteorite samples of angrites are limited to finds, so analysis of an observed fall is not possible in the case of angrites. This raises the question of whether terrestrial weathering had an effect on the Rb isotope composition of SAH 99555 due to the extremely low [Rb] in angrites. Further evidence for this comes from the Rb–Sr chronometer; data show that the Rb–Sr system and highly siderophile elements are disturbed for SAH 99555 and other angrites (Hans et al., 2013; Riches et al., 2012). For these reasons, the most likely explanation for the near-chondritic Rb isotope signature measured in the SAH 99555 is overprinting of any inherent heavy Rb isotope signature by terrestrial Rb. An important future test will be a preliminary sample wash step to remove terrestrial contamination prior to sample dissolution and Rb isotope analysis.

In contrast, heavy Rb isotope enrichments are observed in eucrites and the heated CM relative to chondrites. The two eucrites
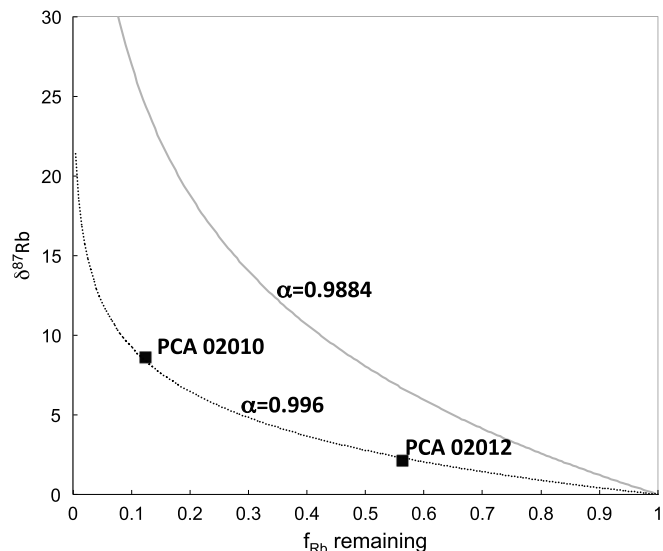

Fig. 6. Plot of δ^{87}Rb versus fraction of Rb remaining in the solid for a typical CM as well as the two heated CM measured in this study (error bars are much smaller than the sample symbols). Shown are the calculated Rayleigh fractionation curve for open system evaporation of Rb (represented by the dotted curve) and the equilibrium evaporation fractionation line (represented by the solid line). The fraction of Rb remaining for the heated CM was calculated by assuming that their initial Rb concentration was that of a typical CM. The heated CM have δ^{87}Rb values that represent $\sim 40\%$ of the ^{87}Rb enrichment predicted by a Rayleigh distillation model.

measured for Rb isotope composition in this study include Juvinas and Stannern, which are both observed falls. These samples have δ^{87}Rb values of $1.51‰$ and $0.55‰$, respectively, and are clearly distinguishable from chondrites. The heated CM display the highest δ^{87}Rb values observed to date for planetary materials, with heavy Rb enrichments of more than $8‰$ on ^{87}Rb/^{85}Rb relative to any of the terrestrial or chondritic samples measured in this study. These samples have lost between 40 and 90% of their Rb, assuming that their initial [Rb] was equal to that of a typical CM. The most likely cause of the heavy Rb isotope enrichments coupled with Rb depletions observed in these samples is volatile loss of Rb during evaporation.

The Rb isotope composition of the heated CM is plotted as a function of fraction of Rb loss in Fig. 6. Also shown are the theoretical Rayleigh distillation curves for open system evaporation of Rb and the equilibrium evaporation fractionation line. The Rayleigh equation is expressed as:

$$\delta^{87}\mathrm{Rb} = \delta^{87}\mathrm{Rb}_0 + \left[\left(1000 + \delta^{87}\mathrm{Rb}_{\mathrm{initial}}\right)\left(F^{\alpha-1} - 1\right) \right] \quad (2)$$

where the 0 superscript indicates the unfractionated material and F is the fraction of initial ^{85}Rb left in the melt. If the isotopic fractionation factor, α, is taken to be (mass of ^{85}Rb/mass of ^{87}Rb)$^{0.5}$ the heated CM have δ^{87}Rb values that approach but do not match those predicted by these theoretical evaporation models. The best matching fractionation factor is 0.996 suggesting that Rb isotope fractionation did not occur under pure vacuum but under partial isotope equilibration between the evaporated gas and the residue. The loss of Rb from a planetesimal requires sufficiently high temperatures to evaporate Rb host phases followed by gravitational escape of Rb. The efficiency of Rb loss may be aided by the incompatible nature of Rb; during silicate differentiation on achondritic parent bodies Rb will be enriched in the surface crustal materials.

Furthermore, the fact that δ^{87}Rb varies by $\sim 1‰$ between the two eucrite samples suggests that the Rb loss rather occurred during planetary processes than during nebular processes (for which an homogeneous Rb isotopic composition for the HED parent body would be expected). This goes in lines with the suggestions that

the volatile loss from the HED parent-body occurred in more oxidizing conditions than the solar nebula based on the variation of the Mn/Na ratio (O'Neill and Palme, 2008).

4.4. Accounting for the similarity in Rb isotopic composition between Earth and chondrites

The general similarity in δ^{87}Rb between the Earth and chondrites (despite the Earth's ∼90% depletion in Rb relative to chondrites) argues against open-system evaporative loss of Rb on Earth. However, early evaporative Rb loss from a proportion of Earth's building blocks before their accretion to Earth is a viable mechanism to create Rb depletions without a significant shift in δ^{87}Rb. As demonstrated by this work, small volatile-depleted bodies initially formed from volatile rich material, but lost volatile elements during accretion. These planetesimals may represent a significant component of the building blocks of Earth, consistent with heterogeneous accretion models (Schönbächler et al., 2010). A mixture of differentiated (δ^{87}Rb > 0, Rb depleted) and chemically primitive (δ^{87}Rb ∼ 0, Rb rich) materials may reproduce the Rb isotope composition and concentration of Earth, since the material with fractionated Rb isotope compositions would be strongly diluted by the chondritic isotopic signature of the volatile-rich material (see also Nebel et al., 2011a).

4.5. The origin of the heavy Rb isotope enrichment in the Moon compared to Earth

This study is the first to reveal a resolvable difference in Rb isotope composition between the silicate Moon and Earth, with lunar rocks enriched in heavy Rb isotopes by 0.2‰ on ^{87}Rb/^{75}Rb. This difference is small but resolvable, and it has important implications for the origins of volatile element depletion in the inner Solar System and for the dynamics of the Moon-forming Giant Impact.

The first case to consider is that the ^{87}Rb enrichment observed in the Moon compared to the Earth is due to non-mass dependent isotope variations, e.g. if the lunar Rb isotope composition is derived from a distinct nucleosynthetic reservoir of Rb and reflects the Rb isotope composition of the impactor rather than the Earth's mantle. In canonical Giant Impact dynamical models the Moon is formed primarily from material sourced from the impactor, rather than from Earth's mantle (Canup, 2014). However, no non-mass dependent differences between the Earth, the Moon, or EC (the proposed compositional analogue for the Moon-forming impactor, Theia) in stable isotope systems have been observed. An exception is the debated small differences in Δ^{17}O (Herwartz et al., 2014; Young et al., 2016). Although bulk meteorites exhibit large variations in stable isotope anomalies of ^{54}Cr and ^{50}Ti, there are no resolvable differences between the ε^{54}Cr or the ε^{50}Ti values of the Earth, the Moon, or EC (Warren, 2011; Dauphas and Schauble, 2016). For this reason, it is unlikely that the heavy Rb isotope enrichments in basalts from the Moon compared to terrestrial basalts is due to the presence of a distinct nucleosynthetic component derived from Theia.

Due to the volatile nature of Rb, one possibility is that the heavy Rb isotope enrichments in lunar basalts compared to terrestrial basalts is due to volatile loss during some stage of the Moon-forming Giant Impact. Further evidence of this should be present in the stable isotope compositions of other elements with a volatility similar to Rb, such as Zn and K. Heavy isotope enrichments in the Moon compared to the Earth are observed for both Zn (by ∼1–2‰ on ^{66}Zn/^{64}Zn) and K (by ∼0.4‰ on ^{41}K/^{39}K); these variations are variously attributed to volatile loss during the Giant Impact (Paniello et al., 2012) or magma ocean degassing in

the case of Zn (Day and Moynier, 2014; Kato et al., 2015) or incomplete condensation from the protolunar disk in the case of K (Wang and Jacobsen, 2016a, 2016b).

No clear correlation is observed between δ^{87}Rb values measured in this study and δ^{66}Zn values measured in lunar samples, likely due to the narrower range in δ^{87}Rb than in δ^{66}Zn (Herzog et al., 2009; Paniello et al., 2012; Kato et al., 2015), although the lunar sample with the lowest δ^{87}Rb value (the high-Ti basalt 10017, δ^{87}Rb = −0.05 ± 0.04‰) is one of the samples that exhibits a very large enrichment in light Zn isotopes (δ^{66}Zn = −5.42‰; Herzog et al., 2009). Although a comparison of the specifics of the isotope data for Rb, K, and Zn does not provide much insight into the cause of positive δ^{87}Rb values in lunar rocks, the identification of heavy isotope enrichments in all three systems is a key indicator that some degree of volatile loss was recorded in the isotope composition of the Moon.

A localized redistribution of Rb due to degassing is unlikely to account for the Rb isotope variations observed in lunar rocks since no complementary lunar reservoir with negative δ^{87}Rb values has been identified at this time; additionally, the plutonic rock analyzed here (norite 77215) also has a heavy δ^{87}Rb value compared to the BSE. The evaporative loss of Rb during either the Giant Impact or the magma ocean stage remains a possibility for generating the heavy Rb enrichment relative to the BSE as long as temperatures are high enough to allow for Rb escape from the Moon. One possibility may be the accretion of volatilized Rb by the Earth during the proto-lunar disk stage following the Giant Impact. The proposal that the K isotope composition of the Moon is created through incomplete condensation from the proto-lunar disk (Wang and Jacobsen, 2016a, 2016b) is dependent on a high energy, high angular momentum Giant Impact in which the Moon-forming material equilibrates with vaporized terrestrial mantle material in a disk that extends outside the Roche limit (Lock et al., 2016). However, this is just one of many proposed dynamical models for the Giant Impact.

However, one important point is that previous stable isotope studies have failed to account for the geochemical processing experienced by Theia (or the precursors of Theia) during accretion prior to the impact event that formed the Moon. It is possible that Theia experienced chemical processing during the early stages of accretion, including silicate differentiation and earlier impact events, resulting in volatile loss and associated heavy isotope enrichments in volatile elements. These geochemical events could modify the chemical and (stable) isotopic composition of Theia but would not affect the nucleosynthetic signature (or lack thereof) that is a key constraint on models of lunar formation. If this is the case, it is possible that the volatile element isotopic composition of the Moon is a memory of the processes experienced by the building blocks of the terrestrial planets during volatile loss in the early Solar System.

5. Conclusions

The Rb isotope compositions of terrestrial rocks define a narrow range in Rb isotope composition, with an average δ^{87}Rb of −0.12 ± 0.06 (2 sd). The homogeneity of δ^{87}Rb values for a variety of terrestrial basalts allows this value to be used as an estimate of the δ^{87}Rb for the BSE.

Carbonaceous chondrites display a trend toward lighter Rb isotope composition coupled with decreasing Rb/Sr, opposite to the effect expected if volatile element abundance variations in CC were caused by evaporation loss of Rb. This relationship indicates that the volatile element abundance variations in CC are not due to evaporation or condensation, but rather are due to the mixing of chemically and isotopically distinct primordial reservoirs.

This study is the first to measure the Rb isotope composition of important examples of volatile-depleted materials, including achondrites and lunar rocks. Significant heavy isotope enrichments on the order of several per mil for ^{87}Rb/^{85}Rb are found for volatile-depleted planetesimals, including eucrites, which display δ^{87}Rb values between 0.5 and 1.5‰. In addition, lunar rocks also display heavy Rb isotope enrichments, with positive δ^{87}Rb shifts of ~0.2‰ compared to the BSE. The most likely cause of these variations in δ^{87}Rb is Rb isotope fractionation due to evaporation during accretion.

Acknowledgements

Appendix A. Supplementary material

Supplementary material related to this article can be found online at http://dx.doi.org/10.1016/j.epsl.2017.05.033.

References

Beck, P., Garenne, A., Quirico, E., Bonal, L., Montes-Hernandez, G., Moynier, F., Schmitt, B., 2014. Transmission infrared spectra (2–25 μm) of carbonaceous chondrites (CI, CM, CV–CK, CR, C2 ungrouped): mineralogy, water, and asteroidal processes. Icarus 229, 263–277. http://dx.doi.org/10.1016/j.icarus.2013.10.019.

Canup, R.M., 2014. Lunar-forming impacts: processes and alternatives. Philos. Trans. R. Soc. A, Math. Phys. Eng. Sci. 372 (2024). http://dx.doi.org/10.1098/rsta.2013.0175.

Dauphas, N., Schauble, E.A., 2016. Mass fractionation laws, mass-independent effects, and isotopic anomalies. Annu. Rev. Earth Planet. Sci. 44, 709–783. http://dx.doi.org/10.1146/annurev-earth-060115-012157.

Day, J.M.D., Moynier, F., 2014. Evaporative fractionation of volatile stable isotopes and their bearing on the origin of the Moon. Philos. Trans. R. Soc. A, Math. Phys. Eng. Sci. 372. http://dx.doi.org/10.1098/rsta.2013.0259.

Halliday, A.N., Porcelli, D., 2001. In search of lost planets – the paleocosmochemistry of the inner solar system. Earth Planet. Sci. Lett. 192 (4), 545–559. http://dx.doi.org/10.1016/S0012-821X(01)00479-4.

Hans, U., Kleine, T., Bourdon, B., 2013. Rb–Sr chronology of volatile depletion in differentiated protoplanets: BABI, ADOR and ALL revisited. Earth Planet. Sci. Lett. 374, 204–214. http://dx.doi.org/10.1016/j.epsl.2013.05.029.

Herwartz, D., Pack, A., Friedrichs, B., Bischoff, A., 2014. Identification of the giant impactor Theia in lunar rocks. Science 344, 1146–1150.

Herzog, G.F., Moynier, F., Albarède, F., Berezhnoy, A.A., 2009. Isotopic and elemental abundances of copper and zinc in lunar samples, Zagami, Pele's hairs, and a terrestrial basalt. Geochim. Cosmochim. Acta 73, 5884–5904. http://dx.doi.org/10.1016/j.gca.2009.05.067.

Hofmann, A.W., 2003. Sampling mantle heterogeneity through oceanic basalts: isotopes and trace elements. In: Treatise on Geochemistry, vol. 2, pp. 61–101.

Humayun, M., Clayton, R.N., 1995. Potassium isotope cosmochemistry: genetic implications of volatile element depletion. Geochim. Cosmochim. Acta 59, 2131–2148. http://dx.doi.org/10.1016/0016-7037(95)00132-8.

Javoy, M., Kaminski, E., Guyot, F., Andrault, D., Sanloup, C., Moreira, M., Labrosse, S., Jambon, A., Agrinier, P., Davaille, A., Jaupart, C., 2010. The chemical composition of the Earth: enstatite chondrite models. Earth Planet. Sci. Lett. 293, 259–268. http://dx.doi.org/10.1016/j.epsl.2010.02.033.

Kato, C., Valdes, M.C., Dhaliwal, J.K., Day, J.M.D., Moynier, F., 2015. Extensive volatile loss during formation and differentiation of the Moon. Nat. Commun. 6, 1–4. http://dx.doi.org/10.1038/ncomms8617.

Larimer, J.W., Anders, E., 1967. Chemical fractionations in meteorites—II. Abundance patterns and their interpretation. Geochim. Cosmochim. Acta 31, 1239–1270. http://dx.doi.org/10.1016/S0016-7037(67)80014-0.

Lock, S.J., Stewart, S.T., Petaev, M.I., Leinhardt, Z.M., Mace, M., Jacobsen, S.B., Ćuk, M., 2016. A new model for lunar origin: equilibration with Earth beyond the hot spin stability limit. In: 47th Lunar and Planetary Science Conference, Abstract 2881.

Lodders, K., 2003. Solar system abundances and condensation temperatures of the elements. Astrophys. J. 591, 1220–1247. http://dx.doi.org/10.1086/375492.

Lodders, K., Fegley Jr., B., 1998. The Planetary Scientist's Companion. Oxford Univ. Press, 371 pp.

Luck, J.-M., Othman, D.B., Albarède, F., 2005. Zn and Cu isotopic variations in chondrites and iron meteorites: early solar nebula reservoirs and parent-body processes. Geochim. Cosmochim. Acta 69, 5351–5363. http://dx.doi.org/10.1016/j.gca.2005.06.018.

Moynier, F., Fegley, B., 2015. The Earth's building blocks. In: Badro, J., Walter, M.J. (Eds.), The Early Earth: Accretion and Differentiation, vol. 212. Wiley, New York, pp. 27–48.

Moynier, F., Paniello, R.C., Gounelle, M., Albarède, F., Beck, P., Podosek, F., Zanda, B., 2011. Nature of volatile depletion and genetic relationships in enstatite chondrites and aubrites inferred from Zn isotopes. Geochim. Cosmochim. Acta 75, 297–307. http://dx.doi.org/10.1016/j.gca.2010.09.022.

Nakato, A., Brearly, A.J., Nakamura, T., Noguchi, T., Ahn, I., Lee, J.I., Matsuoka, M., Sasaki, S., 2013. PCA 02012: a unique thermally metamorphosed carbonaceous chondrite. Lunar Planet. Sci. 44, A2708.

Nebel, O., Mezger, K., Scherer, E.E., Münker, C., 2005. High precision determinations of ^{87}Rb/^{85}Rb in geologic materials by MC-ICP-MS. Int. J. Mass Spectrom. 246, 10–18. http://dx.doi.org/10.1016/j.ijms.2005.08.003.

Nebel, O., Mezger, K., van Westrenen, W., 2011a. Rubidium isotopes in primitive chondrites: constraints on Earth's volatile element depletion and lead isotope evolution. Earth Planet. Sci. Lett. 305, 309–316. http://dx.doi.org/10.1016/j.epsl.2011.03.009.

Nebel, O., Scherer, E.E., Mezger, K., 2011b. Evaluation of the ^{87}Rb decay constant by age comparison against the U–Pb system. Earth Planet. Sci. Lett. 301, 1–8. http://dx.doi.org/10.1016/j.epsl.2010.11.004.

O'Neill, H.S.C., Palme, H., 2008. Collisional erosion and the non-chondritic composition of the terrestrial planets. Philos. Trans. R. Soc. Lond. Ser. A 366, 4205–4238.

Palme, H., Lodders, K., Jones, A., 2014. Solar system abundances of the elements. Treatise on Geochemistry 2, 15–36. http://dx.doi.org/10.1016/B978-0-08-095975-7.00118-2.

Paniello, R.C., Day, J.M.D., Moynier, F., 2012. Zinc isotopic evidence for the origin of the Moon. Nature 490, 376–379. http://dx.doi.org/10.1038/nature1150.

Pringle, E.A., Moynier, F., Beck, P., Paniello, R., Hezel, D.C., 2017. The origin of volatile element depletion in early solar system material: clues from Zn isotopes in chondrules. Earth Planet. Sci. Lett. 468, 62–71.

Riches, A.J.V., Day, J.M.D., Walker, R.J., Simonetti, A., Liu, Y., Neal, C.R., Taylor, L.A., 2012. Rhenium–osmium isotope and highly-siderophile-element abundance systematics of angrite meteorites. Earth Planet. Sci. Lett. 353–354, 208–218.

Ringwood, A.E., 1966. Chemical evolution of the terrestrial planets. Geochim. Cosmochim. Acta 30, 41–104. http://dx.doi.org/10.1016/0016-7037(66)90090-1.

Schönbächler, M., Carlson, R.W., Horan, M.F., Mock, T.D., Hauri, E.H., 2010. Heterogeneous accretion and the moderately volatile element budget of Earth. Science 328, 884–887. http://dx.doi.org/10.1126/science.1186230.

Wang, K., Jacobsen, S.B., 2016a. An estimate of the Bulk Silicate Earth potassium isotopic composition based on MC-ICPMS measurements of basalts. Geochim. Cosmochim. Acta 178, 223–232. http://dx.doi.org/10.1016/j.gca.2015.12.039.

Wang, K., Jacobsen, S.B., 2016b. Potassium isotopic evidence for a high energy giant impact origin of the Moon. Nature 538, 487–490.

Warren, P.H., 2011. Stable-isotopic anomalies and the accretionary assemblage of the Earth and Mars: a subordinate role for carbonaceous chondrites. Earth Planet. Sci. Lett. 311, 93–100. http://dx.doi.org/10.1016/j.epsl.2011.08.047.

Wasson, J.T., Chou, C.-L., 1974. Fractionation of moderately volatile elements in ordinary chondrites. Meteoritics 9, 69–84.

Young, E.D., Kohl, I.E., Warren, P.H., Rubie, D.C., Jacobson, S.A., Morbidelli, A., 2016. Oxygen isotopic evidence for vigorous mixing during the Moon-forming giant impact. Science 351, 493–496. http://dx.doi.org/10.1126/science.aad0525.